

# **ANALYSIS OF VAPOR DENSITY EFFECTS ON HOLD TIMES FOR TOTAL FLOODING CLEAN EXTINGUISHING AGENTS**

Frederick W. Mowrer  
Department of Fire Protection Engineering  
University of Maryland, College Park, MD 20742  
Tel: 301-405-3994; Fax: 301-405-9383; fmowrer@umd.edu

## **Abstract**

Methods to determine leakage rates and agent concentration hold times for clean agent fire suppression systems are addressed in design standards for these systems (e.g., Annex C of NFPA 2001 and Annex E of ISO DIS 14520). These methods are based on well-established theory related to hydrostatic pressure profiles and orifice flow, coupled with fan pressurization measurements and “worst case” assumptions related to leakage path areas and locations. This paper discusses the underlying theory, with an emphasis on agent vapor density effects, and describes a series of experiments that were conducted to compare measured and theoretical leakage rates and hold times for four agents: FK-5-1-12, HFC-227ea, HFC-125 and CO<sub>2</sub>.

## **INTRODUCTION**

Many of the gaseous clean agents being used and considered for use in total flooding fire suppression systems have vapor densities that are significantly higher than that of air. When these agents are injected into enclosures and mixed with air in design concentrations, the density of the agent-air mixture will also be greater than the density of the air in surrounding spaces. This difference in densities between the agent-air mixture within the enclosure and the air in the surrounding spaces results in hydrostatic pressure differences that drive the leakage of the agent-air mixture from the enclosure through leakage paths located low in the enclosure and the flow of air into the enclosure through leakage paths located high in the enclosure. As a result of such leakage, the design agent concentration within the enclosure is maintained only for a period of time, known as the “hold time” or “retention time.”

Hold time refers to the time it takes for the agent concentration to drop below a specified concentration at a designated height. This height is usually the elevation of the highest potential fire source in the enclosure and the concentration is usually taken as 80% of the minimum design concentration [1]. Under current standards the minimum design concentration is typically a factor of 1.2 to 1.3 times the minimum extinguishing concentration [2, 3]. A hold time of at least 10 minutes is generally considered desirable to allow items within the enclosure to cool to prevent re-ignition and also to allow manual suppression forces to arrive to take over suppression activities if necessary.

There are two generally recognized models for leakage flow through enclosure boundaries, the descending interface model and the continuous mixing model. The primary goal of this project is to compare experimentally measured agent concentrations at different elevations with those predicted by the descending interface model. This study evaluates the existing leakage theories

as they apply to the leakage behavior of FK-5-1-12, HFC227ea, HFC125 and CO<sub>2</sub>. An experimental enclosure was constructed to evaluate leakage flows into and out of the enclosure. The effect of different upper and lower leakage areas on the flow characteristics is investigated by varying the leakage areas. Experimental data and theoretical predictions are expressed in dimensionless form to allow comparisons among different enclosure and agent characteristics.

## THEORY

The discharge of a clean agent into an enclosure is highly turbulent and, if properly designed, develops a relatively uniform agent-air mixture throughout the enclosure once the agent discharge is completed. Because most agents have vapor densities greater than that of air, the density of the agent-air mixture is also greater than that of the air surrounding the enclosure. This heavier-than-air mixture exerts a positive hydrostatic pressure on the lower part of the enclosure boundaries. This pressure causes the agent-air mixture to flow out of leakage paths located in the lower part of the enclosure boundaries.

Since the enclosure is of fixed volume the flow of agent-air mixture from lower leakage paths in the enclosure creates a reduced hydrostatic pressure near the top of the enclosure that causes ambient air to flow into the enclosure via leakage paths near the top of the enclosure. The fixed enclosure volume results in a quasi-steady state condition where the volumetric flow rates into and out of the enclosure are equal following an initial transient associated with agent discharge.

A schematic of the hydrostatic pressure profile for a mixture with uniform density in an enclosure is presented in Figure 1. The gray area designates the homogeneous agent-air mixture with density  $\rho_m$ . The height of this mixture,  $h(t)$ , descends as the mixture flows out of the enclosure and ambient air flows in to replace the out-flowing mixture. Figure 1 also schematically shows the presumed inside and outside pressure profiles. A neutral plane at height  $N(t)$  exists at the elevation where inside and outside pressures are the same.

## LEAKAGE AREA AND FLOW RATE

The volumetric flow rates into and out of the enclosure are governed by the hydrostatic pressure differences at the upper and lower leakage paths. These pressure differences are due to density differences between the agent-air mixture and the air surrounding the enclosure. An equation for the volumetric flow rate into or out of an enclosure is expressed as [4]:

$$\dot{V} = C \left( \frac{2\Delta P}{\rho_{air}} \right)^n \quad (1)$$

where  $C = K_d A_T K_u$ . This equation assumes that there are no obstructions near the inlet or outlet, the plate thickness is small compared to the orifice diameter, changes in temperature and absolute pressure are small, and flow through the orifice is turbulent. The constant C is based on the orifice discharge coefficient  $K_d$ , the leakage area  $A_T$ , and a constant  $K_u$  which is based on the value of the flow exponent,  $n$ , and the units being used.  $K_d$  is the ratio of the actual flow to the theoretical maximum flow. This value is taken as 0.61 for sharp-edge circular orifices, the value

used in NFPA 2001 [2]. The value of exponent  $n$  will vary for actual leaks in enclosure boundaries; the value of  $n$  is taken as 0.5, the value used in the current NFPA 2001 standard.

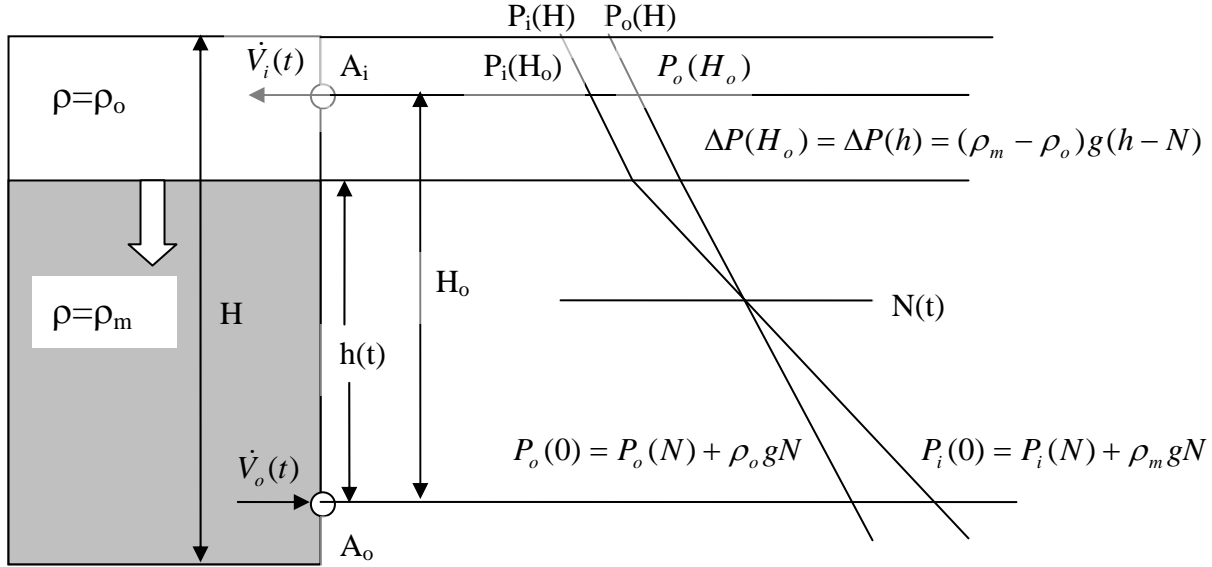


**Figure 1. Hydrostatic Pressure Profile Schematic.**

## FLOW MODELS

There are three generally recognized models for the leakage flow of clean agents: the sharp descending interface model, the continuous mixing model, and the wide interface model. The sharp descending interface and continuous mixing models are described in References 2, 3 and 4. The wide descending interface model was developed more recently by Dewsbury and Whiteley [5]. In this study the descending interface model is investigated. It is expressed in dimensionless terms to permit comparisons over a range of agents and enclosure leakage conditions.

The sharp descending interface model is usually applied to halon alternatives [4] because of their high vapor densities, which give rise to a stably stratified interface between the in-flowing air and the out-flowing agent-air mixture, as depicted in Figure 1. The volumetric flow rates into and out of the enclosure are a function of the leakage areas, the height between upper and lower leakage paths, as well as density differences between the agent-air mixture within the enclosure and the ambient air surrounding the enclosure. The depth of the layer is a major factor governing the flow. A deep layer will create more hydrostatic pressure and as the layer descends, the hydrostatic pressure differences at the lower leakage paths will decrease, reducing the volumetric flow rates over time. An equation relating these volumetric flow rates to the hydrostatic pressure differences within the enclosure are expressed in Equations 2 and 3, respectively.

$$\dot{V}_i = C_i A_i \sqrt{\frac{2\Delta P(h)}{\rho_o}} = C_i A_i \sqrt{\frac{2g(h - N)\Delta\rho}{\rho_o}} \quad (2)$$

$$\dot{V}_o = C_o A_o \sqrt{\frac{2\Delta P(0)}{\rho_m}} = C_o A_o \sqrt{\frac{2gN\Delta\rho}{\rho_m}} \quad (3)$$

A dimensionless expression relating the neutral plane, the height at which there is no hydrostatic pressure difference, to the layer interface height can be found by equating the inlet and outlet flow rates and then rearranging.

$$\frac{N}{h} = \frac{1}{1 + \left(\frac{\rho_o}{\rho_m}\right) \left(\frac{C_o A_o}{C_i A_i}\right)^2} \quad (4)$$

This expression can then be substituted into the volumetric outlet flow rate equation (Equation 3) for a new expression of the volumetric outflow rate as a function of the layer interface height,  $h(t)$ :

$$\dot{V}_o = C_o A_o \sqrt{\frac{2\Delta\rho g h(t)}{\rho_m \left[1 + \left(\frac{\rho_o}{\rho_m}\right) \left(\frac{C_o A_o}{C_i A_i}\right)^2\right]}} = k_1 \sqrt{h(t)} \quad (5)$$

$$\text{where } k_1 = C_o A_o \sqrt{\frac{2\Delta\rho g}{\rho_m \left[1 + \left(\frac{\rho_o}{\rho_m}\right) \left(\frac{C_o A_o}{C_i A_i}\right)^2\right]}} = C_o A_o \sqrt{\frac{2\left(1 - \frac{\rho_o}{\rho_m}\right)g}{\left[1 + \left(\frac{\rho_o}{\rho_m}\right) \left(\frac{C_o A_o}{C_i A_i}\right)^2\right]}}$$

The rate of descent of the interface layer can be represented by the following differential equation, where  $A_c$  is the floor area of the enclosure, assumed to be constant.

$$\frac{dh(t)}{dt} = \frac{-\dot{V}_o(t)}{A_c} = \frac{-k_1}{A_c} \sqrt{h(t)} \quad (6)$$

Equation 6 is integrated from  $H_o$  to  $h(t)$  and from  $t_o$  to  $t$  to determine the elevation of the descending interface as a function of time, where  $t_o$  is the time when the interface reaches  $H_o$ .

$$\int_{H_o}^{h(t)} (h)^{-1/2} dh = \frac{-k_1}{A_c} \int_{t_o}^t dt \Rightarrow \left(\frac{h(t)}{H_o}\right)^{1/2} = 1 - \frac{k_1(t-t_o)}{2A_c\sqrt{H_o}} \quad (7)$$

To nondimensionalize Equation 7, a characteristic volumetric flow rate ( $\dot{V}_c$ ) and a characteristic drain time  $\tau$  are defined, respectively, as:

$$\dot{V}_c \equiv C_o A_o \sqrt{g H_o} \quad (8)$$

$$\tau \equiv \frac{V_o}{\dot{V}_c} = \frac{A_c H_o}{C_o A_o \sqrt{g H_o}} = \left( \frac{A_c}{C_o A_o} \right) \left( \sqrt{\frac{H_o}{g}} \right) \quad (9)$$

When these terms are substituted into Equation 7, the dimensionless form of the interface height is given by Equation 10:

$$\frac{h(t)}{H_o} = \left[ 1 - \frac{k_2(t - t_o)}{\tau} \right]^2 \quad (10)$$

$$\text{where } k_2 = \left[ \frac{\left( 1 - \frac{1}{\tilde{\rho}} \right)}{2 \left( 1 + \frac{1}{\tilde{\rho}} \tilde{A}^2 \right)} \right]^{1/2}, \quad \tilde{\rho} = \frac{\rho_m}{\rho_o} \text{ and } \tilde{A} = \left( \frac{C_o A_o}{C_i A_i} \right).$$

Thus, the parameters governing the rate of descent of the descending interface includes the mixture density relative to the ambient density,  $\tilde{\rho} = \frac{\rho_m}{\rho_o}$ , the ratio between the outlet and inlet

leakage path areas,  $\tilde{A} = \left( \frac{C_o A_o}{C_i A_i} \right)$ , the ratio between the enclosure floor area and the effective

outlet leakage path area,  $\left( \frac{A_c}{C_o A_o} \right)$ , and the height between the inlet and outlet leakage paths,  $H_o$ .

## EXPERIMENTAL SETUP

Experiments were conducted to investigate the flow behavior of clean agents from an enclosure and to compare this behavior with the descending interface model. A test enclosure made out of acrylic plastic was used. The test enclosure was a vertical cylinder with a height of 1.83 m, an inside diameter of 0.61 m and an internal volume of 0.534 m<sup>3</sup>. A number of 12.7 mm diameter holes were drilled into the side of the enclosure for instrumentation and leakage purposes. Three equally-spaced holes were located at a height of 1.68 m to serve as the upper leakage paths. Three holes were located at a height of 0.077 m to serve as the lower leakage paths. These lower and upper leakage areas could be increased or decreased by plugging or unplugging one or more of the holes. A schematic of the test apparatus is shown in Figure 2.

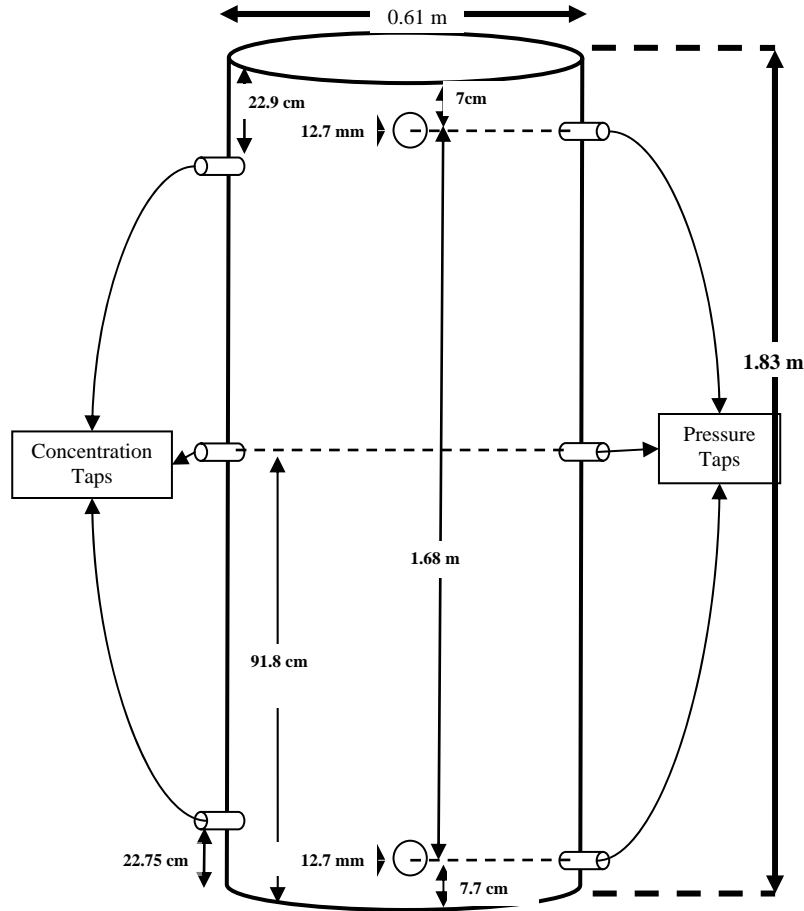


**Figure 2. Schematic of test apparatus, elevation view.**

Three concentration sampling ports were located at 168 cm, 91.8 cm, 23 cm from the base of the enclosure. These ports were connected via plastic tubing to a Tripoint Analyzer which measured the agent concentration at the specified heights during a test. Other instrumentation included three pressure transducers located at 1.68 m, 0.92 m, and 0.15 m above the lower leakage path elevation. These pressure transducers measured the pressure differential between the inside and outside of the enclosure. The upper and lower pressure transducers are located at the same elevations as the upper and lower leakage paths. Type K thermocouples were also placed in the agent discharge stream and in the center of the enclosure to measure the changes in temperature within the enclosure associated with agent discharge and dispersion. A data acquisition unit was used to record all instrumentation measurements during the test at a sampling rate of approximately 1 Hz.

Agent was discharged into the enclosure through a stainless steel sample cylinder and ¼ in NPT stainless steel tubing (ID=9.2 mm). For the halon alternative agents, liquid (FK-5-1-12) or gaseous (HFC227ea or HFC125) agent was added to the sample cylinder, which was then pressurized to approximately 2.48 MPa (360 psig) with nitrogen to represent field conditions. A ball valve isolated the pressurized cylinder from the discharge piping and, when opened, would quickly discharge the agent into the enclosure. Two inline pressure transducers were placed within the discharge piping to measure the pressure. The first was connected to the sample

cylinder to measure its pressure. The second was placed at the fitting connected to the discharge nozzle. A Bete NF1000 discharge nozzle was selected through trial and error so that the discharge time would be approximately 10 seconds per the NFPA 2001 standard. A schematic of the agent delivery system is shown in Figure 3.

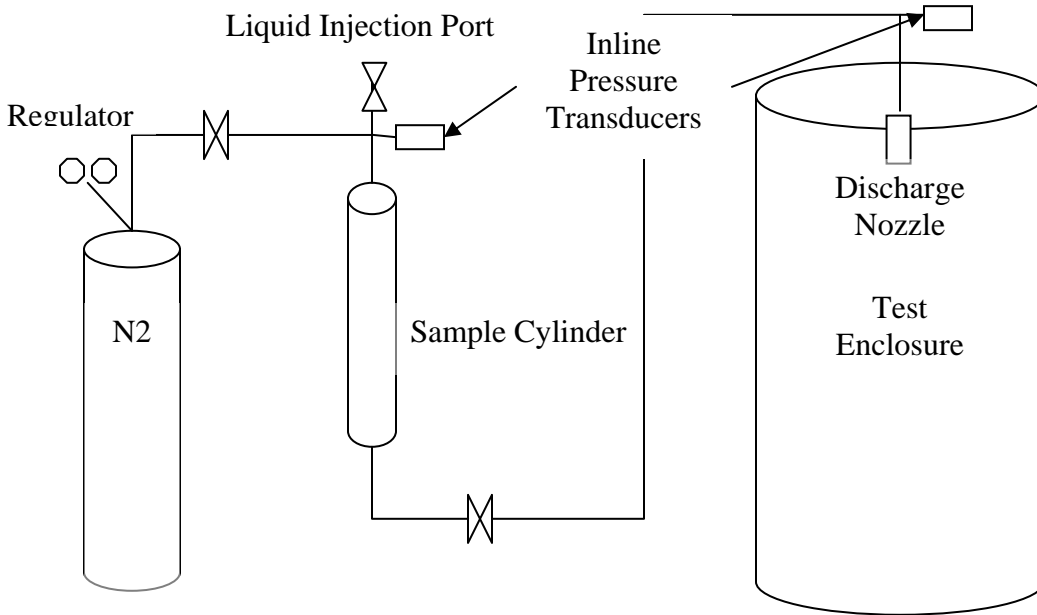


**Figure 3. Schematic of agent delivery system.**

Experiments with five different area leakage scenarios were conducted to investigate the effect of the leakage area and the leakage area ratio on the flow of the agent-air mixture out of the enclosure. The first three sets of experiments had equal upper and lower leakage areas of 3.8 cm<sup>2</sup>, 2.53 cm<sup>2</sup>, and 1.27 cm<sup>2</sup>, respectively. The next set of experiments had an upper leakage area of 3.8 cm<sup>2</sup> and lower leakage area of 1.27 cm<sup>2</sup>. The final set of experiments had an upper leakage area of 1.27 cm<sup>2</sup> and a lower leakage area of 3.8 cm<sup>2</sup>.

In order to validate the leakage area scenarios presented, the ratio of the total leakage area to the surface area of the enclosure can be compared to that found in actual buildings. Klote and Milke [6] characterize the tightness of actual commercial buildings: an area ratio of  $0.50 \times 10^{-4}$  as a tight building,  $0.17 \times 10^{-3}$  as an average building, and  $0.35 \times 10^{-3}$  as a loose building. All of the experiments conducted in this project fall within the range of tight or average tightness based on this definition.

## **EXPERIMENTAL RESULTS**

Agent concentrations and differential pressures between the enclosure and surroundings were the primary measurements made during the experiments. The Tripoint analyzer was used to measure agent concentrations at three elevations approximately every four seconds. These readings

provided a time-concentration profile at elevations of 1.6 m, 0.92 m , and 0.23 m above the base of the chamber. A set of characteristic time-concentration profiles is shown in this section.

Figures 4a and 4b show the time-concentration profile for a discharge test with  $3.8 \text{ cm}^2$  leakage areas in both the upper and lower leakage paths for FK-5-1-12 and HFC227ea, respectively. These graphs support the concept of the descending interface model, at least until the interface descends to the middle sampling port. For the bottom sampling port, these graphs suggest that the descending interface model may no longer be valid.

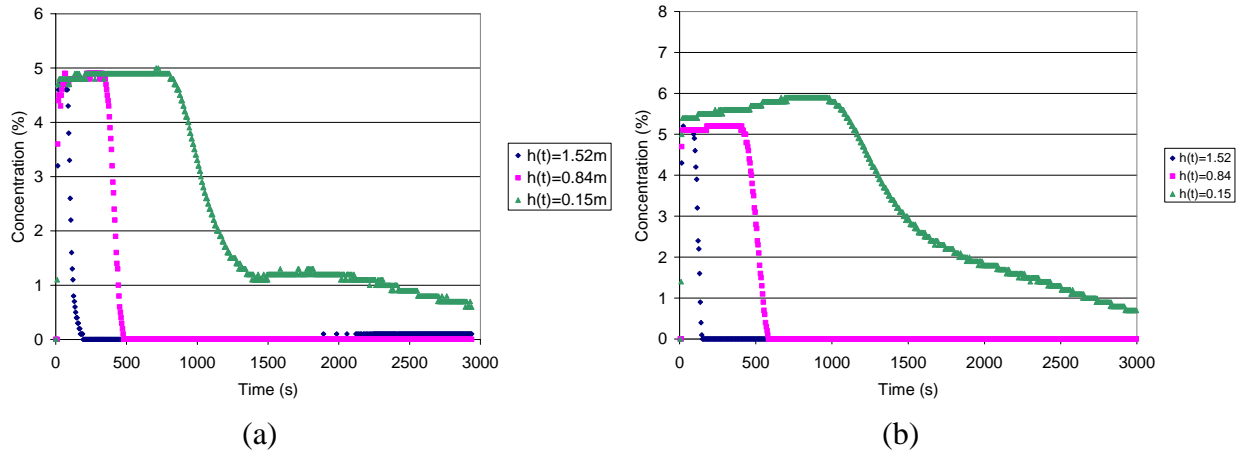


**Figure 4. Time-Concentration profile,  $A_o=A_i=3.8 \text{ cm}^2$ , (a) FK-5-1-12; (b) HFC227ea.**

If the upper and lower leakage areas are equally reduced, the time-concentration profile remains similarly shaped, but the time for the interface to reach each sample elevation increases. Although the hydrostatic driving force remains the same, the area available for leakage decreases, decreasing the volumetric flow rates. Figures 5(a) and 5(b) show the increased hold time for the agent to reach the respective ports as the leakage areas are decreased to  $2.53 \text{ cm}^2$  and  $1.27 \text{ cm}^2$ , respectively.

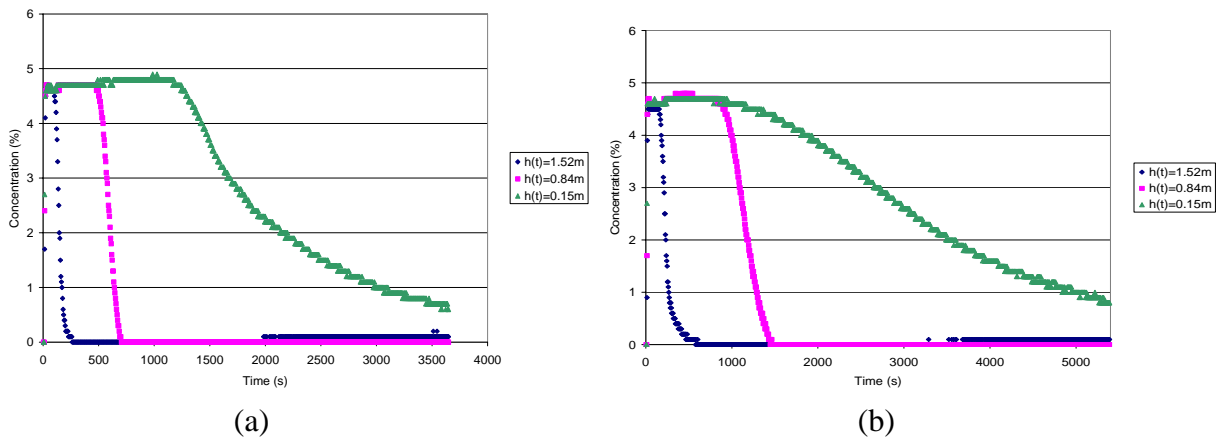


**Figure 5. Time-Concentration profile, FK-5-1-12,  $C_o=4.7\%$ , (a)  $A_o=A_i=2.53 \text{ cm}^2$ , (b)  $A_o=A_i=1.27 \text{ cm}^2$**



Results of experiments with unequal upper and lower leakage areas are shown in Figures 6(a) and 6(b). The case of a leakage area ratio of 0.33 is shown in Figure 6a, while the case of a leakage area ratio of 3 is shown in Figure 6(b). For the first case, the leaks available for flow essentially represent unrestricted inlet flow with restricted outlet flow. These time-concentration profiles are similar to those seen in the equal area case; an interface is formed and the width of the interface increases as the interface descends.

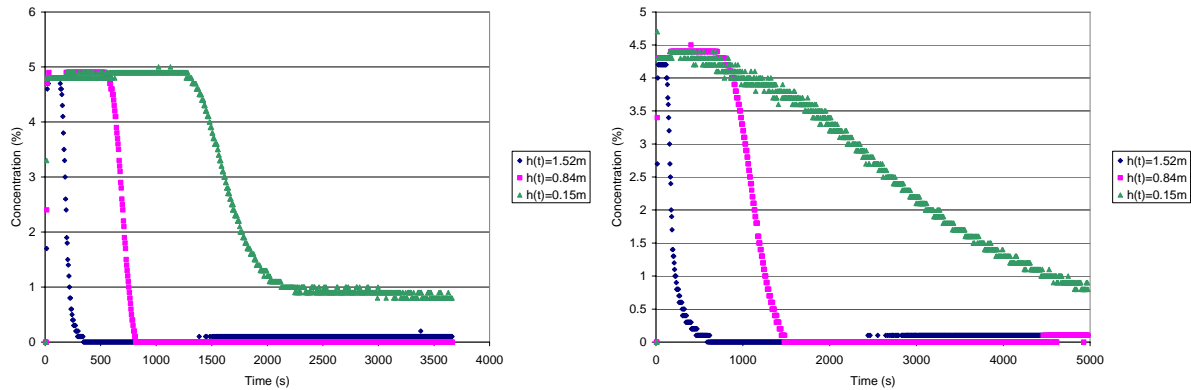


**Figure 6. Time-Concentration profile, FK-5-1-12, (a)  $A_o=1.27 \text{ cm}^2$ ,  $A_i=3.8 \text{ cm}^2$ , (b)  $A_o=3.8 \text{ cm}^2$ ,  $A_i=1.27 \text{ cm}^2$**

For the case of a leakage area ratio of 3, Figure 6(b) shows that a descending interface clearly passes the upper two sample ports. However, similar to the most restricted equal leakage area scenario ( $A_o=A_i=0.000127\text{m}^2$ ), the lowest concentration sample port at a height of 0.22 m shows a time-concentration profile that would be expected more with the continuous mixing model than a sharp descending interface. Because of the limited inlet flow at the top of the enclosure, flow of ambient air into the enclosure may occur at the bottom leakage holes, resulting in bidirectional flow through these paths. This entrainment of ambient air for enclosures with large area ratios was predicted by Dewsbury and Whiteley [1].

Exemplar pressure histories within the test enclosure are shown in Figures 7(a) and 7(b) for a FK-5-1-12 experiment. Figure 7(a) shows the transient pressure behavior during and shortly after agent discharge, while Figure 7(b) shows the slowly changing pressures that occur as the agent-air mixture leaks from the test enclosure. The initial decrease in pressure occurs while the agent is being discharged and vaporizing, an endothermic process that decreases the temperature and pressure within the test enclosure. After this decrease in pressure, there is an increase of pressure due to an increase in volume of the agent-air mixture as it increases from the lower discharge temperature to that of the surroundings (approximately 25°C). As shown in Figure 7(a), these transient pressure pulses only last for approximately 15 seconds, consistent with the agent discharge period.

After this transient behavior, typical hydrostatic pressure profiles exist at the different heights. This behavior is shown in Figure 7(b). At the highest measured point ( $h=1.76\text{m}$ ) there is a negative pressure differential between the enclosure pressure and the ambient air pressure. This

pressure differential is responsible for the entrainment of the fresh air into the enclosure. At the lowest height ( $h=0.077\text{m}$ ) there exists a positive pressure differential, forcing the agent-air mixture out of the enclosure. As the interface layer descends, these pressure differences decrease resulting in a smaller flow rate. These small pressure differences are responsible for the wide interface at the lowest sample port.

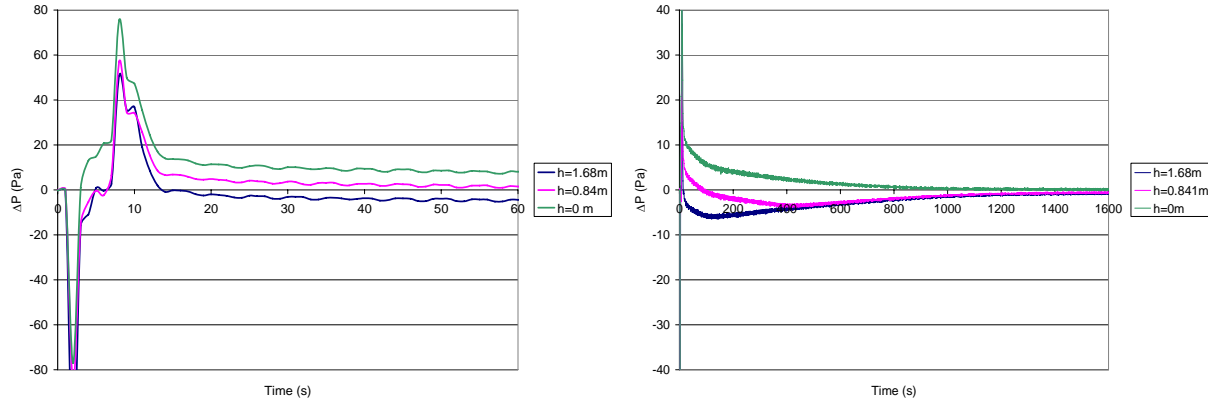


**Figure 7. Hydrostatic Pressure Profiles for a FK-5-1-12 experiment;  $A_o=A_i=0.00038\text{ m}^2$ ;**  
**(a) Initial transient pressures, (b) Long-term pressure profiles.**

## NONDIMENSIONALIZED RESULTS

The hold time of an agent-air mixture within an enclosure is a function of the leakage areas, the mixture density and the height of the descending interface. These parameters will differ between agents and enclosures. In order to compare numerous situations, the hold time experimental results are nondimensionalized and compared with the theoretical results expressed by Equation 10. Figures 8(a) and 8(b) show the dimensionless descending interface height ( $h(t)/H_0$ ) as a function of the dimensionless time ( $k_2(t-t_0)/\tau$ ) for all the experiments, including the FK-5-1-12, HFC-227ea, HFC-125 and  $\text{CO}_2$  experiments, respectively. The experimental data shown is based on the time when the concentration first dropped below 80% of the initial concentration.

Figure 8(a) shows all the experimental data for all four agents and all leakage path configurations. Figure 8(a) shows considerable scatter in the experimental data, particularly for the lowest measurement elevation, where  $h/H_0 = 0.09$ . Figure 8(b) shows the same experimental data, but with data associated with the smallest orifice size ( $A_o$  or  $A_i$  of  $1.27\text{ cm}^2$ ) removed. Figure 8(b) exhibits considerably less scatter in the experimental data, suggesting that the descending interface theory described in this paper may not apply as well for relatively tight enclosures with relatively small leakage paths. Both Figures 8(a) and 8(b) also suggest that the actual rate of agent-air mixture leakage is somewhat faster than predicted by the descending interface theory for the lower two measurement points. Possible reasons for these discrepancies between theory and experiment are still being explored. Potential reasons include temperature effects associated with agent discharge into the enclosure and flow effects associated with agent concentration sampling from the enclosure.

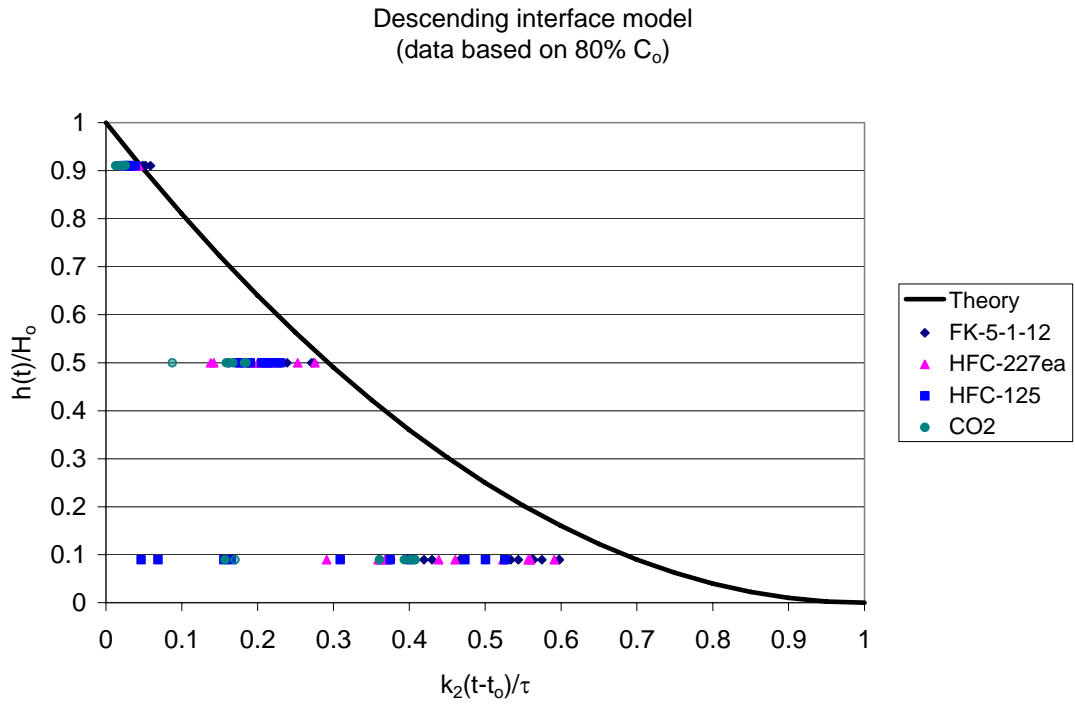


**Figure 8(a). Dimensionless descending interface experimental data  $C=80\% C_o$ , all data.**

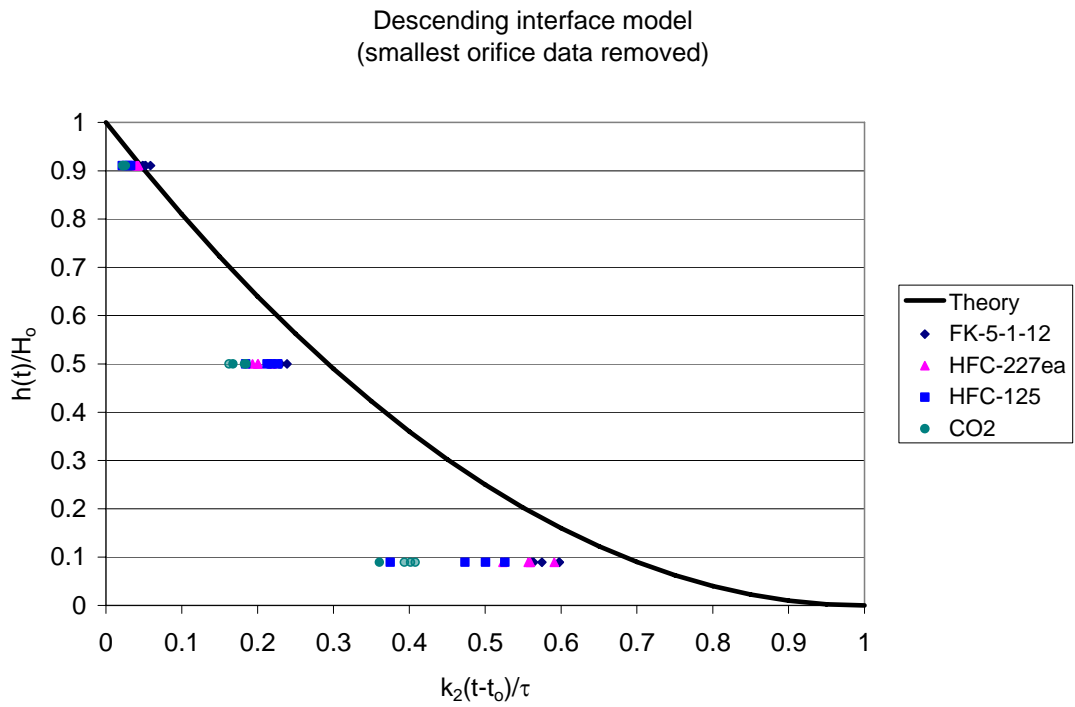


**Figure 8(b) Dimensionless descending interface experimental data  $C=80\% C_o$ , smallest orifice data removed.**

## SUMMARY AND CONCLUSIONS

The main objective of this study was to evaluate experimentally the descending interface model for the flow of fire suppression agent-air mixtures out of enclosures and the resulting hold times. The descending interface model was derived and expressed in dimensionless terms to permit comparisons between theory and experiment for a range of agents and enclosure leakage areas. Thirty-eight experiments were conducted with four agents, FK-5-1-12, HFC-227ea, HFC-125 and CO<sub>2</sub>, for a range of leakage area scenarios. The descending interface model appears to predict the descent of the agent-air mixture interface over the upper half of the enclosure with relatively good accuracy, although the theory appears to over-predict the agent hold time based on the experimental data, as shown in Figure 8(a) and 8(b). Reasons for this are still being considered.

Agent discharge causes negative and positive surges in enclosure pressure during the discharge period. In order for the suppression to be effective, the enclosure needs to be able to withstand these pressure surges. Further analysis of these transient pressure effects on enclosure integrity is warranted.

## REFERENCES

1. Dewsbury J., and Whiteley, R. A., "Review of fan integrity testing and hold time standards," *Fire Technology*, Vol. 36, No. 4, 2000, pp 249- 265.
2. NFPA 2001, *Standard on clean agent fire extinguishing systems*, National Fire Protection Association, 2004.
3. ISO/fDIS 1450.1, *Gaseous fire extinguishing systems – Physical properties and system design, Part 1: General Requirements*, Annex E, International Standards Organization, 2003.
4. DiNenno, P. J., and Forssell, E. W. "Evaluation of the door fan pressurization leakage test method applied to Halon 1301 total flooding systems," *Journal of Fire Protection Engineering*, Vol. 1, No. 4, 1989, pp 131-140.
5. Dewsbury J., and Whiteley, R. A., "Extensions to standard hold time calculations," *Fire Technology*, Vol. 36, No. 4, 2000, pp 266- 278.
6. Klote, J.H and Milke, J.A., *Design of Smoke Management Systems*, ASHRAE, 1992.

## ACKNOWLEDGEMENTS

The assistance of Sean O'Rourke and Jessica Hubert, students in the Department of Fire Protection Engineering at the University of Maryland, in the performance and analysis of the experiments reported here is warmly acknowledged. Financial and technical support provided by 3M for this project is gratefully acknowledged.